

## A marine origin of coal balls in the Midland and Illinois basins, USA

Michelle E. Chrpá <sup>1,2</sup>✉, Anne Raymond <sup>1</sup>, William M. Lamb <sup>1</sup> & Juan-Carlos Laya <sup>1</sup>

Coal balls are carbonate concretions that preserve peat in cellular detail. Despite their importance to paleobotany, the salinity of coal-ball peat remains controversial. Pennsylvanian coal balls from the Midland and Illinois basins contain echinoderms and early high-magnesium calcite cement. Echinoderm skeletons reflect the Mg/Ca ratio of the seawater in which they grew. Here we show that well-preserved echinoderms in coal balls and North American Pennsylvanian marine facies have similar average mole % MgCO<sub>3</sub>; 10.2–12.3 and 9.9–12.5 respectively. Coal-ball echinoderms reflect the magnesium content of the adjacent epicontinental seawater. Early high-magnesium calcite cement in coal balls has the same, or more magnesium than echinoderms from the same deposit, and high Sr/Ca and Na/Ca, consistent with formation in marine or brackish water. Subsequent coal-ball cement is low-magnesium calcite, suggesting freshwater diagenesis and cementation followed formation of marine high-magnesium calcite. Coal balls likely formed in the marine-freshwater mixing zone.

<sup>1</sup>Department of Geology & Geophysics, Texas A&M University, College Station, TX, USA. <sup>2</sup>Department of Earth Sciences, University of Delaware, Newark, DE, USA. ✉email: [mchrpa@udel.edu](mailto:mchrpa@udel.edu)

Coal balls are carbonate concretions in coal or wetland sediments that contain permineralized peat<sup>1</sup> (Fig. 1a). Most come from Pennsylvanian and Permian swamps; however, the environment of coal-ball formation remains controversial<sup>2–5</sup>. Carbon and oxygen stable isotopes appear to support a freshwater origin, along with the habitat of the nearest living relatives of coal-ball plants<sup>4,6,7</sup>. However, in most coal balls with a known paragenetic sequence, the earliest coal-ball cements are high-magnesium calcite (HMC) or non-stoichiometric dolomite, carbonates that occur commonly in marine depositional environments and rarely in freshwater of normal ionic composition<sup>3,4,8–10</sup>. In dolomitic coal balls, subsequent cements are ferroan dolomites, suggesting diagenesis in anoxic marine environments<sup>10</sup>.

In HMC coal balls, subsequent coal-ball cements are low-magnesium calcite (LMC), suggesting initial cementation in marine water followed by cementation and diagenesis in freshwater<sup>2–4</sup>. Within these coal balls, marine (HMC) and freshwater (LMC) cement intermingle, with LMC rimming individual crystals of HMC cement (Fig. 2). Because of this, all coal-ball isotopic studies have sampled a mix of marine and freshwater cement, although Scott and collaborators reported coal-ball carbon and oxygen stable isotopic ratios consistent with formation from a mixture of marine and fresh pore water<sup>2,5</sup>.

Marine facies overlie nearly all Pennsylvanian coals that contain coal balls<sup>1,7,11</sup> (Supplementary Data). In North America, a third of Pennsylvanian transgressive-regressive cycles from the mid-Moscovian through Gzhelian have coals with coal balls<sup>1,12,13</sup>. Of the coals with coal balls, more than 10% have mixed coal balls, which contain plant debris and marine invertebrate fossils including echinoderms<sup>1,12,13</sup>.

Echinoderms are marine organisms that secrete HMC skeletons with distinctive 3D microstructure, called stereom (Fig. 3a–c), which reflects the Mg/Ca ratio of the seawater in which they grew<sup>14,15</sup>. Mg/Ca<sub>C</sub> ratios of echinoderm stereom have

been used to reconstruct the Mg/Ca<sub>SW</sub> ratio of paleo-oceans<sup>15–17</sup>. However, the Mg content of modern seawater varies with temperature, salinity and location, particularly in coastal seas, and this method of predicting global Mg/Ca<sub>SW</sub> ratios has been questioned<sup>18–20</sup>. In this contribution, we use the Mg content of echinoderms from the Late Pennsylvanian Midcontinent Sea (LPMS) of North America as a local indicator of the origin of coal-ball cements in two LPMS coals<sup>21</sup>. Echinoderm fossils in coal balls appear to be stem columnals, probably crinoids. These organisms almost certainly grew in shallow marine environments adjacent to the swamp, and were transported into the swamp where they became incorporated into coal balls. Because of the link between echinoderms and seawater chemistry, echinoderms in coal balls provide new data on pore-water chemistry during coal-ball formation.

We propose and test three hypotheses. One, echinoderm stereom in coal balls records the Mg content of seawater in the epicontinental sea adjacent to the peat swamp. Echinoderms in coal balls likely resulted from storm transport of marine invertebrate shell hash into the peat swamp during storms or due to marine transgression<sup>12,13,22</sup>. If coal-ball echinoderms reflect the Mg/Ca ratio of the LPMS, the Mg content of echinoderm stereom in coal balls should match the Mg content of echinoderm stereom in LPMS marine facies reported by Dickson<sup>15</sup>.

Two, in coal balls with echinoderms and plant-only coal balls from the same locality, early HMC cement formed from marine or brackish pore water should have more Mg than echinoderm stereom. We test this hypothesis by comparing the Mg content of early HMC cement in coal balls to the Mg content of echinoderm stereom in coal balls from the same deposit. Experimental studies show that abiotic cement precipitated from seawater has more Mg than echinoderm stereom grown in seawater of the same composition<sup>23</sup>. Accordingly, coal-ball cement precipitated from marine or brackish water should have the same or higher Mg content as echinoderm stereom precipitated from seawater of the

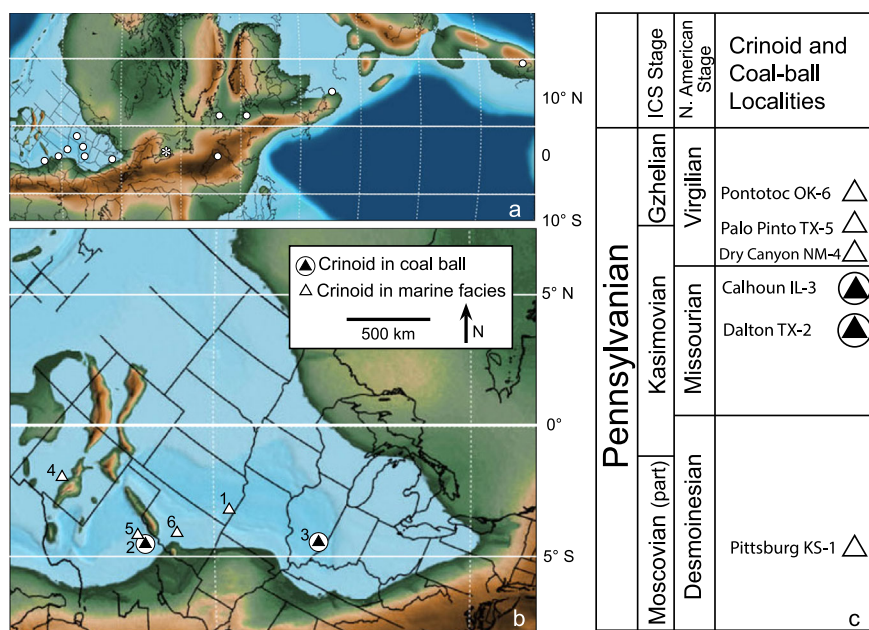


**Fig. 1** Coal ball sample locations and stratigraphic context. **a** Late Pennsylvanian (310 Ma) paleogeographic reconstruction of Scotese (ref. 34) showing Pennsylvanian basins with coal balls (white circles). Supplementary Data documents the presence of marine sediments overlying coals with coal balls, or the presence of marine invertebrates in coal balls in all coalball basins except the Stellarton Basin of Maritime Canada (white asterisk). Partial country boundaries and US state boundaries in black. **b** Late Pennsylvanian (310 Ma) paleogeographic map of North America (ref. 34) showing the location of marine facies as white triangles (ref. 15) and coal balls with echinoderm stereom as black triangles in white circles. Localities: 1—Pittsburg, KS; 2—Dalton coal, Palo Pinto Co., TX; 3—Calhoun Coal, Berryville, IL; 4—Holder Fm., Dry Canyon, NM; 5—Palo Pinto Co., TX; 6—Pontotoc Co., OK. Partial US state boundaries in black. **c** Pennsylvanian stratigraphic column with coal-ball (black triangles in white circles) and marine facies (white triangles) localities.

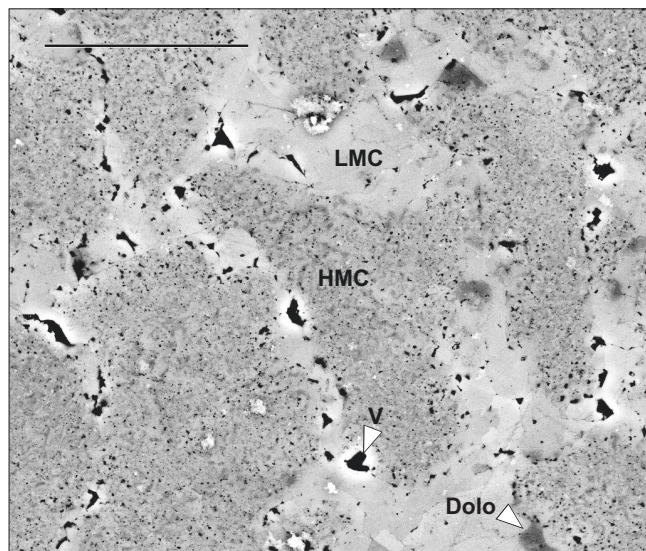


**Fig. 2 BSE image of early HMC cement in plant-only coal ball.** This plant-only coal ball is from the Williamson No. 3 Deposit, Williamson, Iowa, Pennsylvanian (late Atokan - early Desmoinesian; Midcontinent shelf). Columnar crystals of early HMC cement shown here in cross-section, appear speckled in the BSE image. Vuggy LMC (light grey calcite) surrounding the HMC polycrystals results from the diagenetic alteration of HMC. The small dark grey carbonates are non-stoichiometric dolomite crystals. HMC high-magnesium calcite, LMC low-magnesium calcite, V vug, Dolo non-stoichiometric dolomite. The scale is 30  $\mu\text{m}$ . Image taken by Rachel Wells.

same composition. Coal-ball cement precipitated from brackish water would have similar amounts, or slightly less Mg than echinoderm stereom. The Sr and Na content of HMC coal-ball cement provides an additional test of this hypothesis. Cements precipitated from either seawater or brackish water have higher Sr/Ca and Na/Ca values than cements precipitated from freshwater<sup>24</sup>, and should match the ratios of modern marine cement<sup>25</sup>.

Three, fresh pore water replaced marine pore water relatively early in coal ball formation. We test this hypothesis by determining the Mg, Sr and Na content of second-generation calcite cement permineralizing echinoderm stereom and plant debris in coal balls. HMC cements in coal balls also show evidence of early diagenesis in freshwater<sup>3</sup>. Coal-ball cement precipitated from freshwater will have a freshwater Mg signature<sup>26</sup> ( $\leq 5$  mole%  $\text{MgCO}_3$ ), and low Sr/Ca<sub>C</sub> and Na/Ca<sub>C</sub><sup>27</sup>.

In testing our second and third hypotheses, we consider mixed and plant-only coal balls separately. Mixed coal balls, i.e. coal balls with marine invertebrates<sup>12</sup>, often occur at the top of the coal bed and contain fragmented plant debris rather than rooted peat. These coal balls record the Mg/Ca ratio of peat pore water during marine transgression of coastal swamps, and may not reflect the Mg/Ca ratio of pore water during peat accumulation when plant-only coal balls formed. In both types of coal balls, calcite cement precipitated from seawater should have more Mg than echinoderm stereom, and Sr/Ca<sub>C</sub> and Na/Ca<sub>C</sub> indicative of marine HMC cement<sup>17,28</sup>. Coal-ball cement precipitated from brackish water may have similar amounts, or slightly less Mg than echinoderm stereom and higher Sr/Ca<sub>C</sub> and Na/Ca<sub>C</sub> than freshwater cement.

**Sample locations and stratigraphic context.** Coal-balls for this study come from the informally named Dalton coal in Texas (Midland Basin) and the Calhoun Coal of Illinois (Illinois Basin),

both Late Pennsylvanian (Missourian) in age (Fig. 1b, c). The Dalton coal of Texas lies within the Wolf Mountain Shale, and belongs to the Wyandotte Intermediate cycle<sup>1,29,30</sup>. It is underlain by marine shale or thin fossiliferous limestone beds and overlain by calcareous sand or shale<sup>31,32</sup>. Throughout most of its thickness, the Dalton deposit contains limonite (diagenetically altered siderite) concretions; however, coal balls occur at the top 0.3 m of the bed<sup>31</sup>. Plants in Dalton coal balls include tree ferns, medullosan seed ferns, cordaites, and *Calamites*. These coal balls also contain a diverse assemblage of marine invertebrates including crinoids, brachiopods, gastropods, bivalves, and encrusting forams (Fig. 3d).

The Late Pennsylvanian (latest Missourian) Calhoun Coal Member from Berryville, Illinois belongs to the Mattoon Formation of the McLeansboro Group<sup>32</sup>. Overlain by the Omega Limestone Member of the Mattoon Formation, the Calhoun Coal belongs to the Cass cycle<sup>30</sup>. Coal balls occur throughout the deposit but increase in abundance toward the top<sup>12</sup>. Their floral assemblage consists of tree ferns with subdominant seed ferns and lycopsids; their invertebrate assemblage consists of crinoids, brachiopods, bivalves, gastropods and conodonts<sup>12,32,33</sup>.

The Mg content of Missourian crinoids has not been reported, thus we compare the Mg content of coal-ball echinoderms and calcite to the Mg content of echinoderms from the preceding Desmoinesian, and succeeding Virgilian stages<sup>15</sup> (Table 1 and Fig. 1c).

The Late Pennsylvanian (310 Ma) paleogeographic reconstruction places Pennsylvanian basins with coal balls between 0° and 5° paleolatitude<sup>34</sup> (Fig. 1a).

## Results

**Echinoderm Mg, Sr and Na Content.** Late Pennsylvanian echinoderms from marine facies contain 11.0 mole%  $\text{MgCO}_3$  averaged by locality<sup>15</sup>, (range 9.9–12.5 mole%  $\text{MgCO}_3$ ; Table 1). Echinoderm fossils from both the Dalton and Calhoun coals preserve stereom microstructure and yield average Mg values within this range (Fig. 3a–c and Table 1). Neither population differs significantly from echinoderms in Pennsylvanian marine facies; however, Calhoun coal-ball echinoderms (av. 12.3 mole%  $\text{MgCO}_3$ ) have significantly more Mg than Dalton echinoderms (av. 10.2 mole%  $\text{MgCO}_3$ ) (Fig. 4; Supplementary Data). Average Sr/Ca<sub>C</sub> in Dalton and Calhoun coal-ball echinoderms are 1.3 and 1.5 Sr/Ca<sub>C</sub> mmol/mol respectively (Fig. 5a; Table 1). Dalton and Calhoun echinoderm stereom has significantly higher Na/Ca<sub>C</sub> than their interstereom cements (stereom respectively 3.7 and 3.3 Na/Ca<sub>C</sub> mmol/mol; interstereom cement respectively 1.4 and 0.6 Na/Ca<sub>C</sub> mmol/mol; Fig. 6a; Supplementary Data).

For individual ossicles from Dalton coal balls, the average range in Mg/Ca<sub>C</sub> analytic point values (i.e. the difference between the highest and lowest Mg/Ca<sub>C</sub> analytic points measured on each ossicle) is 35 Mg/Ca<sub>C</sub> mmol/mol ( $N = 12$  ossicles; Table 2). For individual ossicles from Calhoun coal balls, the average range in analytic point values is 50 Mg/Ca<sub>C</sub> mmol/mol ( $N = 14$  ossicles; Table 2). The range in average Mg/Ca<sub>C</sub> mmol/mol per ossicle for the Dalton and Calhoun coals are respectively 21 and 68.

**Mg, Sr and Na in early HMC and second-generation LMC cement of coal balls.** Early HMC cement in Dalton mixed coal balls has significantly more Mg than echinoderm stereom from the same coal balls,  $\sim 1.9$  mole%  $\text{MgCO}_3$ . However early HMC cement in Dalton mixed coal balls and Dalton echinoderm stereom contain similar amounts of Mg (Table 1 and Figs. 3e, 4, 5a, b). In the Calhoun, early HMC cement in both mixed and plant-only coal balls has significantly more Mg than echinoderms, respectively 2.5 and 3.5 mole%  $\text{MgCO}_3$  (Table 1 and Figs. 3f, 4, 5). In each deposit,

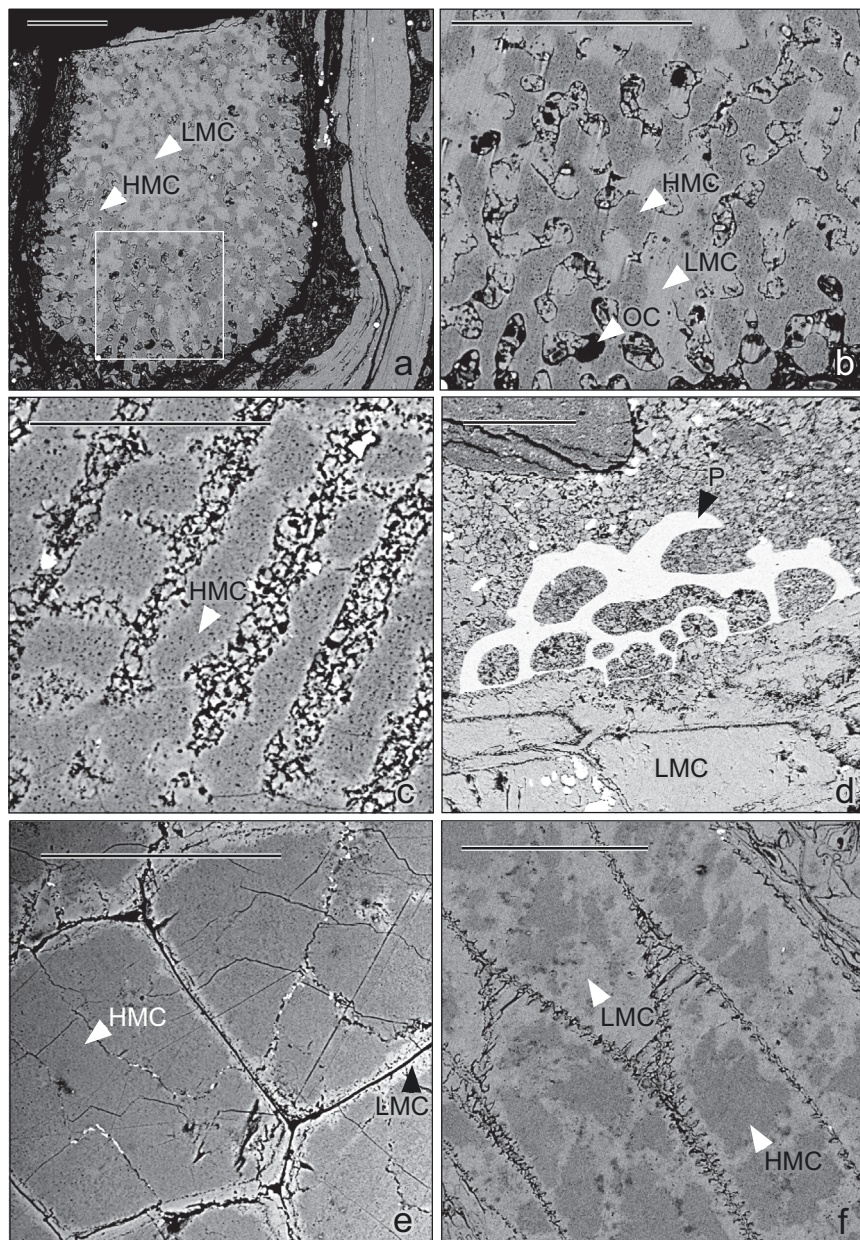


**Fig. 3 BSE images of Dalton and Calhoun coal balls.** 100  $\mu\text{m}$  scale. HMC is medium grey, LMC is light grey and Pyrite (P) is white. **a** Calhoun echinoderm ossicle with stereom microstructure, boxed area enlarged in **b**. **b** Calhoun stereom microstructure enlarged from **a**. Interstereom pores near the lower edge of the image partially filled with black, organic carbon (OC). **c** Dalton echinoderm ossicle with stereom microstructure. Interstereom pores filled with organic carbon (black) and LMC (light grey). **d** Pyritized (P, black arrow) benthic foram growing on root parenchyma cells permineralized with LMC cement, Dalton mixed coal ball. **e** HMC cement in tree-fern root cells, Dalton plant-only coal ball. LMC next to cell walls results from diagenetic alteration of HMC filling cell lumen. **f** HMC and LMC cement in wood cells, Calhoun plant-only coal ball. LMC surrounding cell walls results from the diagenetic alteration of HMC.

echinoderm stereom has significantly more Sr than early HMC cement from both types of coal balls (Table 1 and Fig. 5). Early HMC cement in mixed and plant-only coal balls has significantly higher Na than second-generation LMC (Fig. 6b, c; Supplementary Data).

LMC, most ferroan, some non-ferroan, permineralizes echinoderm stereom in Dalton and Calhoun coal balls (Fig. 3). At each locality, second-generation LMC cement associated with echinoderms and plant debris has a similar amount of Mg (Table 1 and Fig. 5). However, second-generation LMC in plant debris from Dalton plant-echinoderm coal balls has much more Sr than other second-generation LMC (Table 1 and Fig. 5).

**Echinoderm seawater Mg/Ca<sub>sw</sub> ratios.** The predicted Mg/Ca<sub>sw</sub> ratio of Pennsylvanian seawater based on echinoderms in coal balls is 2.8–3.6 mol/mol for the Dalton coal in the Midland Basin and 3.4–4.2 mol/mol for the Calhoun Coal in the Illinois Basin<sup>15</sup> (Table 1).

## Discussion

**Echinoderms in coal balls.** As previously discussed, storms likely transported echinoderm ossicles into the swamp, where they became incorporated into coal balls. The depositional setting and processes that led to the inclusion of echinoderm ossicles in

**Table 1 Magnesium and strontium contents for echinoderms and coal ball calcite.**

Sample type/locality	Age (# localities for marine echinoderms)	Analyses	mole% MgCO <sub>3</sub> Average (range)	Mg/Ca <sub>sw</sub> ratio seawater (mol/mol) Average (range)	Sr/Ca <sub>c</sub> ratio carbonate (mmol/mol) Average (range)
Echinoderms in marine facies, N. Am. Midcontinent shelf*	Desmoinesian (1)	1 ossicle, 10 spots	12.5 (N.A.)	3.7 <sup>†</sup> 5.2 <sup>§</sup>	N.A.
Echinoderms in marine facies, N. Am. Midcontinent shelf*	Virgilian (3)	9 ossicles, 81 spots	10.8 (9.9–11.6)	3.1 (2.8–3.6) <sup>†</sup> 4.2 (3.5–4.9) <sup>§</sup>	N.A.
Echinoderms in marine facies, N. Am. Midcontinent shelf*	Desmoinesian-Virgilian (4)	10 ossicles, 91 spots	11.0 (9.9–12.5)	3.3 (2.8–3.7) <sup>†</sup> 4.3 (3.5–5.2) <sup>§</sup>	N.A.
Echinoderms in echinoderm-plant coal ball, Dalton coal	mid-Missourian	12 ossicles, 85 spots	10.2 (9.4–11.9)	3.0 (2.8–3.6) <sup>†</sup> 3.3 (2.9–4.2) <sup>§</sup>	1.34 (0.99–1.85)
Early HMC cement, echinoderm-plant coal ball, Dalton coal	mid-Missourian	6 plant fossils, 33 spots	11.9 (10.9–12.3)	3.2 (2.8–3.3) <sup>#</sup>	0.70 (0.58–0.88)
Early HMC cement plant-only coal ball, Dalton coal	mid-Missourian	12 plant fossils, 55 spots	10.5 (8.8–12.0)	2.7 (2.1–3.1) <sup>#</sup>	0.84 (0.70–1.04)
LMC cement in echinoderms, Dalton coal	mid-Missourian	7 ossicles, 14 spots	2.4 (2.0–3.5)	N.A.	0.74 (0.54–0.88)
LMC cement in plant debris plant-echinoderm coal ball, Dalton	mid-Missourian	7 plant fossils, 37 spots	2.1 (1.5–2.5)	N.A.	2.89 (0.60–4.98)
LMC cement in plant fossil plant-only echinoderm ball, Dalton	mid-Missourian	10 plant fossils, 31 spots	1.7 (1.2–2.2)	N.A.	0.66 (0.38–1.00)
Echinoderm in echinoderm-plant coal ball, Calhoun Coal	latest Missourian	14 ossicles, 90 spots	12.5 (11.2–13.2)	3.7 (3.3–4.0) <sup>†</sup> 4.5 (3.8–5.1) <sup>§</sup>	1.54 (1.28–1.97)
Early HMC cement, echinoderm-plant coal ball, Calhoun Coal	latest Missourian	6 plant fossils, 13 spots	14.8 (12.6–17.5)	4.2 (3.4–5.2) <sup>#</sup>	0.97 (0.54–1.23)
Early HMC cement, plant-only coal ball, Calhoun Coal	latest Missourian	10 plant fossils, 44 spots	15.8 (13.1–17.8)	4.5 (3.5–5.3) <sup>#</sup>	0.70 (0.49–1.19)
LMC cement in echinoderms Calhoun Coal	latest Missourian	13 ossicles, 43 spots	2.3 (1.0–4.0)	N.A.	1.11 (0.33–1.74)
LMC cement in plant debris plant-echinoderm coal ball, Calhoun	latest Missourian	8 plant fossils, 19 spots	2.8 (1.9–4.1)	N.A.	1.55 (0.92–2.14)
LMC cement in plant fossil plant-only coal ball, Calhoun	latest Missourian	7 plant fossils, 11 spots	1.6 (0.7–2.1)	N.A.	0.24 (0.00–0.24)

Seawater Mg/Ca<sub>sw</sub> mol/mol calculated using partition coefficient  $D^{Mg} = 0.03757$  (ref. 15) and power partition functions  $Mg/Ca_c = 0.0516Mg/Ca_{sw}^{0.668}$ ,  $Mg/Ca_c = 0.0482Mg/Ca_{sw}^{0.898}$  (ref. 28).  
\* Data from Dickson (ref. 15), averaged by locality.  
<sup>†</sup> Mg/Ca ratio calculated with partition coefficient  $D^{Mg} = 0.03757$  (ref. 15).  
<sup>§</sup> Mg/Ca ratio calculated with power partition function  $Mg/Ca_c = 0.0516Mg/Ca_{sw}^{0.668}$  (ref. 28).  
<sup>#</sup> Mg/Ca ratio calculated with power partition function  $Mg/Ca_c = 0.0482Mg/Ca_{sw}^{0.898}$  (ref. 28).

Pennsylvanian coal balls may be similar to the ones that led to the inclusion of Cretaceous crinoids in Burmese amber<sup>35</sup>. Cementation of the stereom probably occurred in the swamp. The interstereom cement matches the composition of the second generation of coal-ball cement, with the exception of high Sr/Ca<sub>c</sub>, which may be due to aragonite dissolution in fresh pore water. Further, echinoderms in both deposits show evidence of infiltration by peat organic fluids into the interstereom pore space prior to cementation (Figs. 3a–c and 7d). These ossicles have coal-filled interstereom pores. The LMC cement of other coal-ball echinoderm ossicles has void spaces, also suggesting the presence of peat organic fluid in the interstereom pores prior to cementation (Figs. 3a–c and 7c). Coal-ball ossicles frequently have borings, and ossicle fragments in coal balls may result from the breakage of bored ossicles (Fig. 7b, d). Nonetheless, some echinoderm ossicles in coal balls have diagenetic histories similar to those preserved in marine facies. For example, a number of coal-ball ossicles have Dickson's type 1 preservation on the edge, and type 2 in the middle<sup>15</sup> (Fig. 7e). Although we use analytical points collected from the edge of these ossicles, we did not use analytical points from regions with type 2 preservation (Figs. 3a–c and 7).

**Mg, Sr and Na in LPMS echinoderms.** The echinoderms from marine facies used in this study come from the LPMS<sup>15</sup> and contain 9.9–12.5 mole% MgCO<sub>3</sub> (Table 1 and Fig. 1b). The amount of Mg incorporated into HMC increases with temperature and decreases with freshwater influx<sup>14,19</sup>. Variations in temperature, depth and proximity to the shoreline, as well as diet and vital effects, could contribute to this range in Mg content<sup>18,36–38</sup>.

The average Mg content of both Dalton and Calhoun echinoderms is statistically indistinguishable from values reported for echinoderms from Pennsylvanian LPMS marine facies<sup>15</sup> (Table 1). This result supports our first hypothesis, echinoderms in coal balls retain the Mg/Ca ratio of the seawater in which they grew, even when transported to, and preserved in, peat swamps. However, Calhoun echinoderms from the Illinois Basin contain significantly more Mg than Dalton echinoderms from the Midland Basin (Figs. 1b, 4, 5a and Table 1). Vital effects or environmental variation tied to basin depth, evaporation and higher water temperature could contribute to more Mg in Calhoun echinoderms<sup>14,18,19,36–38</sup>.

Samples of echinoderm ossicles from a single locality yield similar ranges in Mg/Ca<sub>c</sub> (~21–85 mmol/mol), regardless of geological age (Table 2). The Dalton coal has a narrow range in average ossicle Mg/Ca<sub>c</sub>, 21 mmol/mol, whereas the Calhoun Coal and samples of Recent crinoids from the Bahama Banks and Suruga Bay, Japan have larger ranges in average ossicle Mg/Ca<sub>c</sub> between 65–85 mmol/mol<sup>39</sup> (Table 2). Data from Recent crinoids suggest that we should expect a wide range in estimates of ancient seawater Mg/Ca based on the Mg/Ca<sub>c</sub> of echinoderm stereom.

One modern crinoid ossicle yields a wide estimated range of Mg/Ca<sub>c</sub> values (154 mmol/mol Mg/Ca<sub>c</sub>, 1.44 wt% Mg), possibly due to variations in the composition of the associated organic matrix<sup>37,39</sup>. Because very few fossil crinoids retain biomolecules<sup>40,41</sup>, the range of Mg/Ca<sub>c</sub> values observed in Dalton and Calhoun ossicles probably results from both diagenesis and the vital effects rather than variation in the composition of the associated organic matrix. Both freshwater and marine diagenesis of HMC results in loss of Mg and Sr ions, producing LMC<sup>42</sup>. Thus, Mg/Ca<sub>c</sub> values of ancient

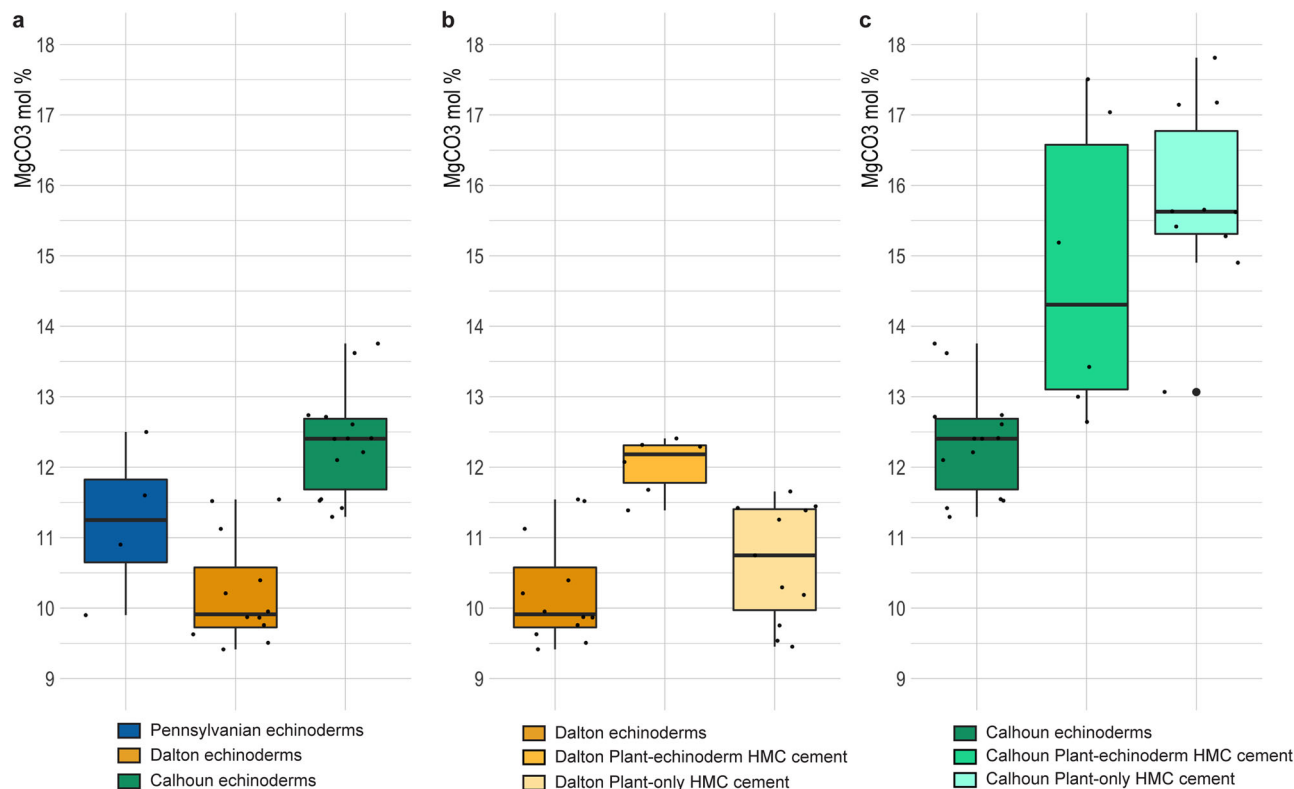


**Fig. 4** Box plots showing the distribution of mole%  $\text{MgCO}_3$  values among Pennsylvanian echinoderms from marine facies (ref.<sup>15</sup>), coal-ball echinoderms and HMC cement from the Dalton and Calhoun coals. **a** Echinoderms from Pennsylvanian marine facies (ref.<sup>15</sup>), Dalton coal, and Calhoun Coal. **b** Dalton echinoderms and HMC cements from mixed and plant-only coal balls. **c** Calhoun echinoderms and HMC cements from mixed and plant-only coal balls. For all box plots, the boxes extend from the upper and lower quartiles (interquartile range, Q3 to Q1), the horizontal solid black line is the median. Whiskers extend from boxes out to 1.5 times the interquartile range. Data points are shown in small, black circles. Any data past the ends of the whiskers are outliers and shown as large, black circles.

echinoderm stereom likely underestimate the  $\text{Mg}/\text{Ca}_{\text{SW}}$  of the water in which the stereom formed.

Variable  $\text{Mg}/\text{Ca}_C$  values in fossil echinoderms are consistent with BSE images of ancient echinoderm stereom that show a mottled pattern of darker ( $>\text{Mg}$ ) and lighter ( $<\text{Mg}$ ) carbonates<sup>43</sup> (Fig. 3b, c). Modern echinoderm stereom has narrow edges of lower Mg carbonate 1–2  $\mu\text{m}$  wide adjacent to the interstereom pores and fairly uniform Mg content in the middle<sup>18,43</sup>. Dickson hypothesized that early interstereom cement acted as a ‘crystal casket’, inhibiting loss of Mg ions from HMC stereom<sup>43</sup>. Although HMC calcite readily transforms into dolomite and LMC, Dickson proposed that the Mg content of the original HMC could be modeled if the volume and  $\text{Mg}/\text{Ca}$  of the dolomite and calcite were known<sup>43,44</sup>. Nonetheless, we did not collect points from stereom with nearby non-stoichiometric dolomite crystals.

The average  $\text{Sr}/\text{Ca}_C$  mmol/mol of coal-ball echinoderms, 1.34 for in the Dalton and 1.54 in the Calhoun, is significantly higher than the  $\text{Sr}/\text{Ca}$  ratio of early HMC cement in mixed and plant-only coal balls (Table 1; Fig. 6a; Supplementary Data). High rates of stereom formation relative to abiotic precipitation rates may facilitate the incorporation of minor and trace elements in skeletal calcite<sup>24,45</sup>. Modern echinoderms have higher  $\text{Sr}/\text{Ca}_C$  than LPMS echinoderms, ranging from 1.6 in echinoids from the Arctic and the NW Atlantic to nearly 5 in holothurians from the NE Atlantic<sup>46,47</sup>. Although coal-ball echinoderms have significantly higher  $\text{Na}/\text{Ca}_C$  than their interstereom cement, coal-ball echinoderms have low  $\text{Na}/\text{Ca}_C$  compared to modern echinoderms. Whereas Dalton and Calhoun echinoderms have average  $\text{Na}/\text{Ca}_C$  of 3.7 and 3.3 mmol/mol, respectively,  $\text{Na}/\text{Ca}_C$  of modern

Arctic echinoderms ranges from 57 to 93 mmol/mol<sup>47</sup>. Loss of Na during burial diagenesis may account for low  $\text{Na}/\text{Ca}_C$  ratios in Pennsylvanian echinoderms<sup>48</sup>.

**Early HMC cements.** The echinoderms in Dalton and Calhoun coal balls likely grew in marine, shallow-shelf communities adjacent to the peat swamp and washed on to the peat surface during storms. Well-preserved stereom in coal-ball echinoderms reflects the  $\text{Mg}/\text{Ca}$  of the LPMS seawater in which they grew. The  $\text{Mg}/\text{Ca}_C$  of early HMC cement in Dalton and Calhoun coal balls suggests this cement formed from marine pore water<sup>49</sup> (Fig. 5b, c and Table 1). This HMC cement has higher  $\text{Mg}/\text{Ca}_C$  than well-preserved echinoderm stereom from the same coal balls, consistent with echinoderm growth and coal-ball formation from marine water with similar  $\text{Mg}/\text{Ca}_{\text{SW}}$  (Figs. 4, 5 and Table 1). The relationship between  $\text{Mg}/\text{Ca}_C$  in early HMC coal-ball cement and echinoderm stereom from the same coal balls (higher in coal balls, lower in echinoderms) supports our second hypothesis, the early HMC cement of coal balls formed from marine pore water. In the Calhoun deposit, both mixed and plant-only coal balls likely formed from marine pore water (Figs. 4, 5 and Table 1). In the Dalton deposit, mixed coal balls probably formed from marine water, whereas plant-only coal balls, which have HMC cement with  $\text{Mg}/\text{Ca}_C$  matching that of Dalton echinoderms, likely formed from brackish water (Figs. 4, 5 and Table 1). Nonetheless, both types of Dalton coal balls yield similar predicted seawater  $\text{Mg}/\text{Ca}_{\text{SW}}$  (Table 1).

Early HMC cements in coal balls have been attributed to microbial precipitation of HMC in freshwater peat due to carbonate springs<sup>4</sup>. However, with averages of 10.5–15.8 mole%

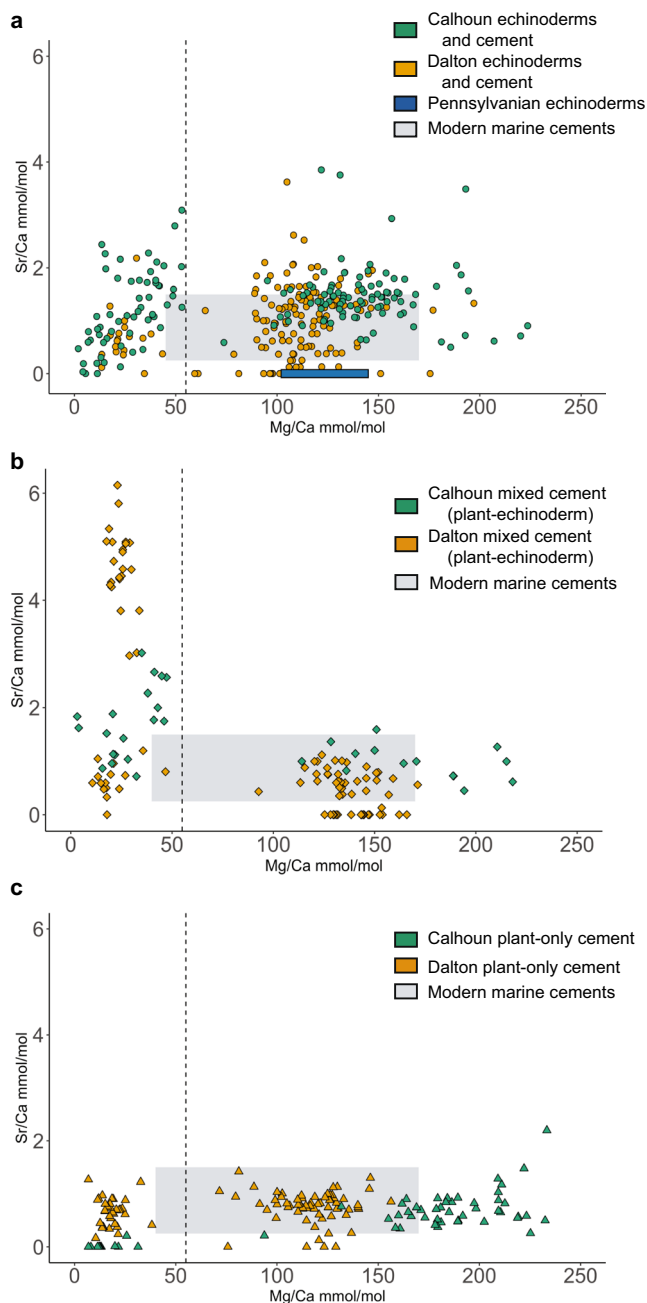


**Fig. 5 Cross-plots of Sr/Ca<sub>c</sub> and Mg/Ca<sub>c</sub> for coal-ball and echinoderm calcite.** Sr/Ca<sub>c</sub> and Mg/Ca<sub>c</sub> for coal-ball and echinoderm calcite are shown in comparison to modern marine cement (ref. 25). Dashed line at 55 Mg/Ca separates LMC values to the left and HMC values to the right. Calhoun values are green and Dalton values are orange. **a** Coal-ball echinoderms and interstereom cement in mixed echinoderm-plant coal balls (circles) Mg/Ca<sub>c</sub> of Pennsylvania marine echinoderms (blue bar) (ref. 15). **b** Plant calcite in mixed echinoderm-plant coal balls (diamonds). **c** Plant calcite in plant-only coal balls (triangles). All ratios were reported in mmol/mol.

MgCO<sub>3</sub>, the early HMC cements of Dalton and Calhoun coal balls have far more Mg than most freshwater calcite (≤5 mole% MgCO<sub>3</sub>; ref. 26), with the exception of HMC formed in hypersaline, alkaline lakes, or lakes in carbonate terrains with seasonally dry climate<sup>50–52</sup>. None of these modern lakes is currently the site of peat accumulation. Further, the columnar crystal habit of early HMC cement in all coal balls suggests an abiotic origin<sup>4,53</sup>.

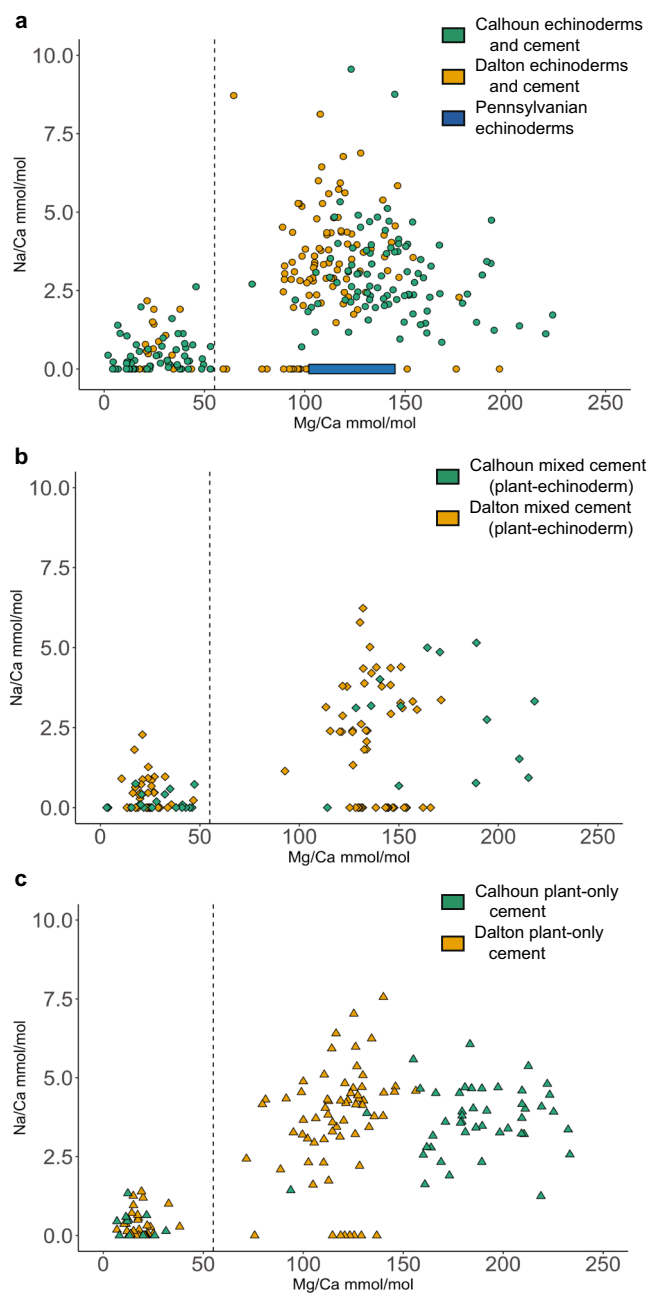


**Fig. 6 Cross-plots of Na/Ca<sub>c</sub> and Mg/Ca<sub>c</sub> for coal-ball and echinoderm calcite.** The dashed line at 55 Mg/Ca separates LMC values to the left and HMC values to the right. Calhoun values are green and Dalton values are orange. **a** Coal-ball echinoderms and interstereom cement in mixed echinoderm-plant coal balls (circles) Mg/Ca<sub>c</sub> of Pennsylvania marine echinoderms (blue bar) (ref. 15). **b** Plant calcite in mixed echinoderm-plant coal balls (diamonds). **c** Plant calcite in plant-only coal balls (triangles). All ratios were reported in mmol/mol.

**Second-generation LMC cements.** Second-generation carbonate cement permineralizing echinoderm stereom and plants in coal balls is usually ferroan LMC. This cement may indicate the presence of fresh, low-Mg pore water in the wetland during coal-ball formation<sup>3,5</sup>, supporting our third hypothesis, fresh pore water replaced marine pore water relatively early in coal-ball formation. This would place the environment of coal-ball formation in the marine/freshwater mixing zone<sup>2</sup> (Table 1). LMC in coal balls results from both cementation and diagenesis of HMC polycrystals<sup>3</sup> (Figs. 2 and 3d). A coal ball from the Herrin Coal in

**Table 2 Comparison of range in Mg/Ca<sub>C</sub> mmol/mol for Pennsylvanian echinoderm ossicles and modern crinoid ossicles (ref. 39).**

Locality	Age	Number of ossicles	Average Mg/Ca <sub>C</sub> for locality (range) (mmol/mol)	Range Mg/Ca <sub>C</sub> of ossicles by site (mmol/mol)	Average range of Mg/Ca <sub>C</sub> analytic point values per ossicle (mmol/mol)
Dalton coal	Pennsylvanian	12	114 (105–126)	21	35
Calhoun Coal	Pennsylvanian	14	144 (130–198)	68	50
Bahama Banks*	Recent	41	145 (114–179)	65	89†
Suruga Bay*	Recent	45	142 (111–196)	85	131†

\*Data from Gorzelak et al. (ref. 39).

†estimated by pairing highest wt% Ca with lowest wt% Mg and lowest wt% Ca with highest wt% Mg.

the Illinois Basin shows evidence of three generations of early HMC cement, separated by thin layers of ferroan, LMC cement<sup>4</sup>, suggesting that fresh pore water replaced marine pore water twice during its formation.

Low Na/Ca<sub>C</sub> values in second-generation LMC cement also support a freshwater origin for this calcite, or freshwater diagenesis of marine carbonate (Fig. 6). Experimental results suggest that the Na content of calcite increases rapidly with increasing salinity of the aqueous solution up to ~10 psu<sup>54</sup>. Above 10 psu, the Na content of calcite increases slowly with increasing salinity<sup>54</sup>. In addition to the Na content of water, the growth rate of calcite crystals also influences their Na/Ca ratio, such that rapidly growing crystals have higher Na/Ca<sub>C</sub> than slowly growing crystals in seawater of the same salinity<sup>55</sup>. Thus while calcite with high Na/Ca<sub>C</sub> ratios indicates precipitation in brackish or marine water, Na/Ca<sub>C</sub> values do not allow precise salinity predictions within this range<sup>54,55</sup>. Likewise, freshwater diagenesis of marine carbonate also decreases its Na content<sup>27,56</sup>, which may account for low Na/Ca<sub>C</sub> values in second-generation LMC.

**Aragonite dissolution during coal-ball formation.** The Sr/Ca<sub>C</sub> in coal-ball cements may reflect aragonite dissolution during coal-ball formation. Aragonite formed in equilibrium with seawater contains ~10,000 ppm Sr; whereas calcite formed in equilibrium with seawater contains ~1000 ppm Sr<sup>27</sup>. Thus, high Sr/Ca<sub>C</sub> ratios in calcite cement may signal precipitation in the presence of dissolving aragonite<sup>49</sup>. Plant-only coal balls from the Dalton and Calhoun localities show no evidence of aragonite dissolution during their formation. In these coal balls, both the early HMC cement and the second-generation LMC have modest Sr/Ca<sub>C</sub>, ranging below the detection limit (0.02 wt% Sr) to 2.2 mmol/mol (Fig. 6c).

Mixed coal balls from both deposits show an interesting pattern of Sr/Ca<sub>C</sub>. In both, early HMC cement has modest Sr/Ca<sub>C</sub>, ranging from 0.1 mmol/mol, which is above the detection limit for Sr, to 1.6 mmol/mol, suggesting no dissolution of aragonite occurred during the formation of this cement, consistent with precipitation from marine pore water (Fig. 6b). However, LMC cement from both deposits has elevated Sr/Ca<sub>C</sub>, slightly so in the case of Calhoun (0.7–3.1 mmol/mol; Fig. 6b), greatly so in the case of the Dalton (0.3–6.1 mmol/mol; Fig. 6b). Elevated Sr/Ca<sub>C</sub> values in second-generation LMC cement, may indicate aragonite dissolution in the swamp during precipitation of LMC cement. Both processes could result from the presence of fresh pore water in the swamp. All the LMC cement in Calhoun mixed coal balls (i.e. LMC cement in plant debris and the interstereom pores of ossicles) has a similar range of Sr/Ca<sub>C</sub> (Fig. 6b). However, in Dalton mixed coal balls, a single sample of LMC from the interstereom pore space has elevated Sr/Ca<sub>C</sub> (Fig. 6b).

Elevated Sr/Ca<sub>C</sub> (>1.5 mmol/mol) in second-generation LMC may indicate the presence of marine aragonite in the swamp prior

to coal-ball formation even in the absence of marine fossils. Many discussions of coal-ball formation suggested that the dissolution of marine carbonate shells contributed to the formation of coal balls<sup>5,6,12,57,58</sup>. Sr/Ca<sub>C</sub> in coal-ball cement provides a test of this hypothesis.

**Late Pennsylvanian midcontinent seawater Mg/Ca<sub>SW</sub> ratios.** All of the echinoderm fossils that Dickson used to predict Pennsylvanian Mg/Ca<sub>SW</sub> came from the LPMS, and Pennsylvanian echinoderms from LPMS coal balls yield significantly similar Mg/Ca<sub>SW</sub> values, suggesting that fossil echinoderms from the same time interval and epicontinental sea may enable us to trace relative changes in Phanerozoic Mg/Ca<sub>SW</sub><sup>15</sup> (Table 1; Supplementary data). However, echinoderm stereom and coal-ball HMC cement from the Midland Basin (Dalton coal) contain significantly less Mg than comparable populations from the Illinois Basin (Calhoun Coal; Table 1, Supplementary Data). Vital effects or differences in water depth leading to more evaporation, or higher water temperature could lead to more Mg in HMC from the Illinois Basin. Understanding whether we can use fossil echinoderms to track the history of Mg/Ca in seawater may require studies that incorporate multiple samples from the same basin, and which track Mg/Ca<sub>C</sub> in more than one basin from each time interval<sup>21</sup>.

**Coal-ball carbonates as environmental archives.** Coal-ball cements are environmental archives of wetland conditions during formation and early diagenesis; as for all carbonates, the trace and minor elemental composition of coal-ball cement provides clues to pore water salinity and oxygen availability during carbonate precipitation and diagenesis<sup>3,10</sup>. Stopes and Watson were among the first to propose that Pennsylvanian coal balls with HMC or dolomite cement formed in marine swamps<sup>3,8,10</sup>. The relative Mg/Ca<sub>C</sub> values of early HMC cement and echinoderm fossils in Dalton and Calhoun coal balls are consistent with the formation of these coal balls in marine or brackish swamps. In all HMC or dolomitic coal balls, the first carbonate cements formed in oxic environments, whereas second-generation cements usually formed in anoxic conditions<sup>3,4,10</sup>.

The presence of marine sediments overlying nearly all coal beds that contain coal balls is consistent with their formation in marine peat (dolomitic coal balls) or in marine or brackish peat, close to the marine-freshwater mixing zone (early HMC, second-generation LMC coal balls; Supplementary Data). However, more paragenetic sequence data are needed to determine whether this is a widespread pattern. Coal balls with LMC or siderite as the first widespread carbonate cement, may have formed in freshwater. For example, sideritic coal balls from the Foord seam in the Stellarton Basin of Canada, overlain by lacustrine sediments, may have formed in freshwater swamps<sup>59–62</sup>. The first widespread carbonate cement in these coal balls is low-Mg siderite, indicative of anoxic, freshwater environments<sup>59,62</sup>. Subsequent generations



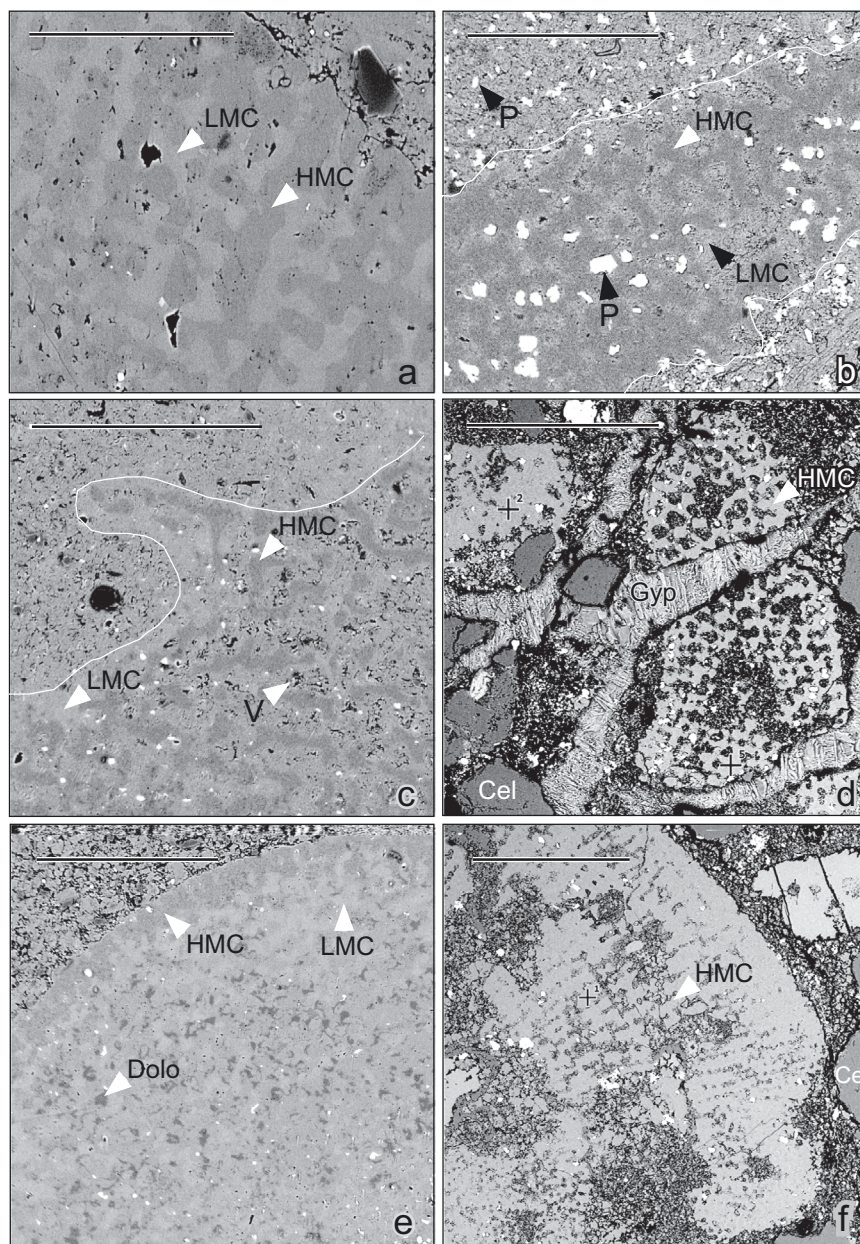


**Fig. 7 BSE images of echinoderm ossicles from Calhoun and Dalton coal balls.** Each image is from an echinoderm used in this study unless noted. **a** Well-preserved Calhoun ossicle showing HMC stereom in medium grey and LMC interstereom cement in light grey. The scale is 100  $\mu\text{m}$ . **b** Relatively well-preserved Dalton ossicle fragment outlined in white, surrounded by LMC coal-ball cement at the top of the image. HMC stereom medium grey, LMC interstereom cement light grey, pyrite (P) white. The scale is 200  $\mu\text{m}$ . **c** Relatively well-preserved Calhoun ossicle fragment outlined in white surrounded by LMC coal-ball cement. HMC stereom medium grey, LMC interstereom cement light grey, V, vugs in LMC interstereom cement. The scale is 200  $\mu\text{m}$ . **d** Broken Dalton ossicle cut by gypsum vein (Gyp), not used in this study. HMC stereom (medium grey) filled with organic carbon (black), pyrite (P) (white) and small carbonate grains. The lower cross shows the location of EDS (energy-dispersive spectroscopy) analysis indicating HMC stereom. The upper cross shows the location of EDS analysis of a second ossicle fragment indicating HMC stereom. Strontium sulfate (Cel) dark grey. Scale is 300  $\mu\text{m}$ . **e** Calhoun ossicle with Dickson type 1 (Gorzalak type 0) preservation on the rim and Dickson type 2 (Gorzalak type 2) preservation in the middle, HMC stereom medium grey, LMC interstereom cement light grey, dolomite (Dolo) dark grey (refs. <sup>15,18</sup>). Scale is 200  $\mu\text{m}$ ; **f** Bored Dalton ossicle with stereom not used in this study. White Arrow indicates HMC stereom, cross shows location of EDS analysis indicating HMC stereom. The scale is 300  $\mu\text{m}$ .

of carbonate cement are Mg-carbonates, dolomite and ankerite, although the source of the Mg-laden pore water in a lacustrine basin remains unexplored<sup>62</sup>.

Retallack<sup>11</sup> described carbonate nodules with permineralized plants and freshwater snails from the Hitchcox limey (fen) peat on the south coast of Australia. These nodules formed in Recent peat that has accumulated behind coastal dunes, underlain by Miocene limestone and limestone soils on the landward side. The

Miocene limestone and carbonate nodules from this site reveal similar stable isotopic patterns, consistent with both pedogenic carbonate and freshwater diagenesis of marine limestone<sup>11</sup>. The carbonate mineralogy and paragenetic sequence of these nodules, which would enable us to test hypotheses of their formation, has not been reported<sup>11</sup>.

Although coal balls with early HMC or dolomite cement indicate the presence of marine or brackish peat swamps, even in

coals with coal balls, their occurrence is sporadic<sup>1</sup>. Most Late Paleozoic paleotropical coal accumulated in freshwater. Nonetheless, our results suggest that equatorial mangrove swamps may be a more appropriate environmental analogue for coal-ball peat than tropical freshwater swamps. This idea has implications for our understanding of late Paleozoic land-plant communities. Whereas freshwater peat swamps are among the least productive land-plant communities in the tropics today, mangroves are among the most<sup>63–66</sup>. In addition to gradients in water depth, nutrients and climate, gradients in salinity probably affected species distributions in coal balls. If coal balls preserve brackish and marine plant communities, yet most Late Paleozoic paleotropical coal formed from freshwater peat, this may help to explain why few coal-ball communities match the palynomorph diversity of their source coal<sup>67–70</sup>.

## Conclusions

The Mg content of early HMC cement in Dalton and Calhoun coal balls (8.8–17.8 mole% MgCO<sub>3</sub>) matches or exceeds the Mg content of echinoderm ossicles from the same localities (9.4–13.2 mole% MgCO<sub>3</sub>), suggesting that coal-ball formation began in marine or brackish water. Echinoderm stereom in coal balls is permineralized by ferroan and non-ferroan LMC, suggesting that second-generation coal-ball calcite formed from fresh pore water, usually anoxic but occasionally oxic, confirming freshwater presence in the swamp relatively early in coal-ball formation, and supporting coal-ball formation close to the peat surface. Coal balls likely formed in coastal swamps, in the mixing zone between marine and fresh pore water. Elevated Sr levels in the second-generation LMC of plant-echinoderm coal balls may derive from dissolution of aragonitic shell material and sediment, and could be a way to trace the presence of marine aragonite during coal-ball formation.

## Methods

**Sample preparation and structural analysis.** Initially, we characterised samples using optical and electron (SEM/EDS) microscopy. In order to obtain Mg/Ca<sub>C</sub> ratio data, we sliced Dalton and Calhoun coal balls and prepared thin sections from these slices. We identified echinoderm ossicles in thin sections using a Zeiss Axioplan 2 microscope and attached AxioCam HRC digital camera. We used a Phenom XL scanning electron microscope (SEM) equipped with energy-dispersive spectroscopy (EDS) to acquire secondary- and backscattered-electron (BSE) images, as well as EDS spectra on selected calcites (typical operating conditions consisted of an accelerating voltage of 15 kV and a working distance of 4 to 8 mm). The images and spectra enabled us to identify targets for electron microprobe (EMP) analysis.

Echinoderm ossicles in coal balls often display patchy preservation, with areas of well-preserved stereom composed of HMC and poorly-preserved areas with indistinct stereom (Figs. 3a–c and 7). All echinoderm analytical points came from stereom with type 1 diagenetic transformation, in which stereom may appear speckled in backscattered-electron (BSE) images due to the formation of dolomite microcrystals, but is distinct from the permineralizing cement<sup>18,43</sup> (Figs. 3a–c, 7). This preservation type encompasses the type 0 and 1 transformations of Gorzelak and collaborators<sup>18</sup>. Early HMC cement in coal balls displays a similar speckled texture in BSE images<sup>3</sup> (Fig. 2).

**Electron microprobe (EMP) geochemical analysis.** We perform chemical characterisation of carbonates using wavelength dispersive (WDS) analyses with a Cameca SX-5, housed in the Texas A&M - the Materials Characterization Facility (MCF) Core Facility (RRID:SCR\_022202). These analyses allow us to characterise the Calcium, Magnesium, Strontium, Iron, Sodium, Manganese, Sulfur, Silicon and Aluminum contents of echinoderm ossicles and plant cements. Operating conditions consisted of an accelerating voltage of 15 kV and a beam current of 10 nA. The diameter of the electron beam at the sample (spot size) was 5 µm, and counting times ranged from 20–30 s for most elements and 40 s for strontium. Detection limits are Mg – 200 ppm, Sr – 260 ppm, Fe – 400 ppm, and Mn – 360 ppm. We used natural and synthetic mineral standards for calibration and time-dependent intensity (TDI) corrections were applied to standards and unknowns<sup>71</sup>.

EMP characterisation of calcite chemistries targets echinoderm ossicles with preserved stereom microstructure in polished, carbon-coated thin sections: all echinoderm analytical points in this study come from areas of the ossicle with clear

stereom microstructure (Figs. 3a–c and 7). We analyze HMC cement and echinoderm ossicles from the same coal ball to create a dataset of paired echinoderm ossicle and coal-ball HMC cement mole% MgCO<sub>3</sub> values. Following previous work<sup>15</sup>, in mixed coal-balls from each locality, we choose 12–15 ossicles, collecting 3–12 analytical points from each ossicle (seven ossicles with 3–12 data points for the Dry Canyon, NM crinoid study<sup>43</sup>). In the same coal balls from each locality, we identify 6–8 plant fragments and collect 2–12 analytical points from each, depending on the size of the fragment. In mixed coal balls, we target *Psaronius* (tree-fern) root fragments and small pieces of wood for microprobe analysis of calcite cement. In plant-only coal balls from each locality, we identify 10–12 locations and collect 2–10 analytical points from each. In plant-only coal balls, we targeted roots and void spaces between pieces of plant debris for microprobe analysis of calcite cement. Typically, analytic points were selected based on greyscale BSE images where HMC and LMC were identified respectively as “dark” and “light”. Early HMC cements in coal balls are polycrystals that display similar speckled texture in BSE images (Fig. 3). Ca, Mg, Sr and Na elemental data (wt%) appear in the Supplementary Data.

We discarded analytic points with weight percent (wt%) totals outside the 98–102% window<sup>71–73</sup>. We also discarded analytic points in echinoderm stereom and early HMC cement with >5000 ppm Fe (>0.5 wt% Fe). Modern echinoderm skeletons have from 100–2300 ppm Fe; the crinoid *Antedon mediterranea* has from 800–1800 ppm Fe<sup>46</sup>. Likewise, the early HMC cement of coal balls is non-ferroan<sup>3,4</sup>. More than 5000 ppm Fe in either type of HMC signals diagenetic alteration, which may have affected the Mg/Ca<sub>C</sub><sup>74</sup>.

**Mg/Ca ratio nomenclature.** We follow previous workers in reporting the Mg/Ca ratio of seawater (Mg/Ca<sub>SW</sub>) as a molar (mol/mol) ratio<sup>15,17,18,21,23,28,75</sup>. However, methods of reporting the Mg/Ca ratio of calcite (Mg/Ca<sub>C</sub>) vary. Here, we report the Mg content of calcite both as mole% MgCO<sub>3</sub>, to facilitate comparisons to previous work by Dickson<sup>15</sup>, and as the ratio of mmol Mg to mol Ca (Mg/Ca<sub>C</sub>) to simplify comparison of our results to those of other workers<sup>19,49</sup>. We report mole% MgCO<sub>3</sub>, Mg/Ca<sub>SW</sub> (mmol/mol), Sr/Ca<sub>C</sub> (mmol/mol), and Na/Ca<sub>C</sub> (mmol/mol), in Table 1 and Supplementary Data.

A number of definitions have been proposed for LMC and HMC, LMC <4 mol % MgCO<sub>3</sub> or LMC <5 mol % MgCO<sub>3</sub>, and HMC >8 mol % MgCO<sub>3</sub><sup>24,26,76</sup>. Because mol % MgCO<sub>3</sub> values for calcite depend on knowing the concentrations of other important minor and trace elements in calcite, these do not easily translate into Mg/Ca mmol/mol values. For the purpose of this contribution, we consider Mg/Ca ≥55 mmol/mol as HMC.

**Statistical analysis.** We test for statistically significant differences in Mg and Sr content among sample populations of echinoderm stereom using the Mann–Whitney *U*-test<sup>77</sup>. To establish the Mg/Ca<sub>C</sub> content of mid-to-late Pennsylvanian echinoderms from the LPMS, we use four locality averages (Pittsburg, KS; Pontotoc Co., OK; Palo Pinto Co., TX; Holder Fm., Dry Canyon, NM; Fig. 1b, c) from existing Pennsylvanian echinoderm stereom data<sup>15</sup>. We determine coal-ball ossicle averages for both the Dalton coal and Calhoun Coal separately. For each coal-ball locality, we test for statistically significant differences and similarities in Mg, Sr and Na among three populations of HMC (stereom in mixed coal balls, and early HMC cement in mixed and plant-only coal balls), and three populations of second-generation calcite (in echinoderm stereom, and in plant debris from mixed and plant-only coal balls). A summary of results appears in the Supplementary Data.

**Mg seawater partitioning.** We use the partition coefficient  $D^{\text{Mg}} = 0.03757$  for echinoderms<sup>15</sup>, and power partition functions  $\text{Mg}/\text{Ca}_C = 0.0516 \text{Mg}/\text{Ca}_{\text{SW}}^{0.668}$  for echinoderms and  $\text{Mg}/\text{Ca}_C = 0.0482 \text{Mg}/\text{Ca}_{\text{SW}}^{0.898}$  for calcite cement<sup>28</sup>, to calculate the Mg/Ca<sub>SW</sub> ratio of Late Pennsylvanian seawater on the Midcontinent Shelf and in the Illinois Basin from HMC in echinoderms and coal-ball cement<sup>75</sup>. Results for Mg/Ca<sub>SW</sub> (mol/mol) estimates appear in Table 1 and Supplementary Data.

## Data availability

Data for this study are accessible at figshare: <https://doi.org/10.6084/m9.figshare.22812749>.

Received: 16 August 2022; Accepted: 2 June 2023;

Published online: 15 June 2023

## References

1. Raymond, A., Lambert, L. L. & Costanza, S. H. Are coal balls rare? A cyclostratigraphic analysis of coal-ball occurrence in North America. *Int. J. Coal Geol.* **206**, 65–79 (2019).
2. Scott, A. C., Matthey, D. P. & Howard, R. New data on the formation of Carboniferous coal balls. *Rev. Palaeobot. Palynol.* **93**, 317–331 (1996).

3. Raymond, A., Guillemette, R., Jones, C. P. & Ahr, W. M. Carbonate petrology and geochemistry of Pennsylvanian coal balls from the Kalo Formation of Iowa. *Int. J. Coal Geol.* **94**, 137–149 (2012).
4. Siewers, F. D. & Phillips, T. L. Petrography and microanalysis of Pennsylvanian coal-ball concretions (Herrin Coal, Illinois Basin, USA): Bearing on fossil plant preservation and coal-ball origins. *Sediment. Geol.* **329**, 130–148 (2015).
5. Breecker, D. O. & Royer, D. L. The pedogenic formation of coal balls by CO<sub>2</sub> degassing through the rootlets of arborescent lycopsids. *Am. J. Sci.* **319**, 529–548 (2019).
6. Anderson, T. F., Brownlee, M. E. & Phillips, T. L. A stable isotope study on the origin of permineralized peat zones in the Herrin Coal. *J. Geol.* **88**, 713–722 (1980).
7. Demaris, P. J. Formation and distribution of coal balls in the Herrin Coal (Pennsylvanian), Franklin County, Illinois Basin, USA. *J. Geol. Soc.* **157**, 221–228 (2000).
8. Stopes, M. C. & Watson, D. M. S. On the present distribution and origin of the calcareous concretions in coal seams, known as “Coal Balls”. *Philos. Trans. R. Soc. Lond. Ser. B Contain. Pap. Biol. Character* **200**, 167–218 (1909).
9. Garrels, R. & Wollast, R. Equilibrium criteria for two-component solids reacting with fixed composition in an aqueous phase; example, the magnesian calcites; discussion. *Am. J. Sci.* **278**, 1469–1474 (1978).
10. Richter, D. K. et al. First description of Phanerozoic radial fibrous dolomite. *Sediment. Geol.* **304**, 1–10 (2014).
11. Retallack, G. Modern analogs reveal the origin of Carboniferous coal balls. *Palaeogeogr. Palaeoclimatol. Palaeoecol.* **564**, 110185 (2021).
12. Mamay, S. H. & Yochelson, E. L. Occurrence and Significance of Marine Animal Remains in American Coal Balls. *U.S. geol. Surv. Prof. Pap.* **354**, 193–224 (1962).
13. Perkins, T. W. Textures and conditions of formation of Middle Pennsylvanian coal balls, central United States. *Univ. Kans. Paleontol. Contrib.* **82**, 1–13 (1976).
14. Mackenzie, F. T. et al. in *Carbonates* (ed. Reeder, R. J.) Ch. 4 (De Gruyter, 1983).
15. Dickson, J. A. D. Echinoderm skeletal preservation: calcite-aragonite seas and the Mg/Ca ratio of phanerozoic oceans. *J. Sediment. Res.* **74**, 355–365 (2004).
16. Dickson, J. A. D. Paleozoic Mg calcite preserved: Implications for the Carboniferous ocean. *Geology* **23**, 535 (1995).
17. Dickson, J. A. D. Fossil echinoderms as monitor of the Mg/Ca ratio of Phanerozoic oceans. *Science* **298**, 1222–1224 (2002).
18. Gorzelak, P., Krzykowski, T. & Stolarski, J. Diagenesis of echinoderm skeletons: constraints on paleoseawater Mg/Ca reconstructions. *Glob. Planet. Change* **144**, 142–157 (2016).
19. Lebrato, M. et al. Global variability in seawater Mg:Ca and Sr:Ca ratios in the modern ocean. *Proc. Natl. Acad. Sci. USA* **117**, 22281–22292 (2020).
20. Gorzelak, P. et al. A Devonian crinoid with a diamond microlattice. *Proc. R. Soc. B Biol. Sci.* **290**, 20230092 (2023).
21. Kolbuk, D., Dubois, P., Stolarski, J. & Gorzelak, P. Impact of seawater Mg<sup>2+</sup>/Ca<sup>2+</sup> on Mg/Ca of a sterozoan skeleton – Evidence from culturing and the fossil record. *Chem. Geol.* **584**, 120557 (2021).
22. Moore, L. R. Some Sediments Closely Associated with Coal Seams in *Coal and Coal-Bearing Strata* (eds. Murchison, D. G. & Westoll, T. S.) 105–123 (Oliver and Boyd, 1968).
23. Ries, J. B. Review: geological and experimental evidence for secular variation in seawater Mg/Ca (calcite-aragonite seas) and its effects on marine biological calcification. *Biogeochemistry* **7**, 2795–2849 (2010).
24. Carpenter, S. J. & Lohmann, K. C. Sr/Mg ratios of modern marine calcite: Empirical indicators of ocean chemistry and precipitation rate. *Geochim. Cosmochim. Acta* **56**, 1837–1849 (1992).
25. Major, R. P. & Wilber, R. J. Crystal habit, geochemistry, and cathodoluminescence of magnesian calcite marine cements from the lower slope of Little Bahama Bank. *Geol. Soc. Am. Bull.* **103**, 461–471 (1991).
26. Burton, E. A. & Walter, L. M. Relative precipitation rates of aragonite and Mg calcite from seawater: temperature or carbonate ion control? *Geology* **15**, 111 (1987).
27. Veizer, J. Chemical diagenesis of carbonates: theory and application of trace element technique, in *Stable Isotopes in Sedimentary Geology SEPM Short Course Notes* (Eds. Arthur, M. A., Anderson, T. F., Kaplan, I. R., Veizer, J. & Land, L. S.) **10**, 3.1–3.100 (SEPM, 1983).
28. Ries, J. B. Effect of ambient Mg/Ca ratio on Mg fractionation in calcareous marine invertebrates: a record of the oceanic Mg/Ca ratio over the Phanerozoic. *Geology* **32**, 981 (2004).
29. Boardman, D. R. & Heckel, P. H. Glacial-eustatic sea-level curve for early Late Pennsylvanian sequence in north-central Texas and biostratigraphic correlation with curve for midcontinent North America. *Geology* **17**, 802 (1989).
30. Heckel, P. H. Pennsylvanian stratigraphy of Northern Midcontinent Shelf and biostratigraphic correlation of cyclotheles. *Stratigraphy* **10**, 3–39 (2013).
31. Lowenstein, G. R. *The Environment of Deposition of the Dalton Coal (Upper Pennsylvanian), Palo Pinto Co., TX* (Texas A&M University, 1986).
32. Willard, D. A., Phillips, T. L., Lesnikowska, A. D. & DiMichele, W. A. Paleocology of the Late Pennsylvanian-age Calhoun coal bed and implications for long-term dynamics of wetland ecosystems. *Int. J. Coal Geol.* **69**, 21–54 (2007).
33. Phillips, T. L. Stratigraphic occurrences and vegetational patterns of Pennsylvanian pteridosperms in Euramerican coal swamps. *Rev. Palaeobot. Palynol.* **32**, 5–26 (1981).
34. Scotese, C. PALEOMAP PaleAtlas for GPlates and the PaleoData Plotter Program, PALEOMAP Project. <https://doi.org/10.1130/abs/2016NC-275387> (2016).
35. Salamon, M. A. et al. Paleoenvironmental and biostratigraphic implications of echinoderm ossicles trapped within Burmese amber. *PALAIOS* **34**, 652–656 (2019).
36. Kolbuk, D. et al. Effects of seawater Mg<sup>2+</sup>/Ca<sup>2+</sup> ratio and diet on the biomineralization and growth of sea urchins and the relevance of fossil echinoderms to paleoenvironmental reconstructions. *Geobiology* **18**, 710–724 (2020).
37. Hermans, J., André, L., Navez, J., Pernet, P. & Dubois, P. Relative influences of solution composition and presence of intracrystalline proteins on magnesium incorporation in calcium carbonate minerals: Insight into vital effects. *J. Geophys. Res.* **116**, G01001 (2011).
38. Weber, J. N. The incorporation of magnesium into the skeletal calcites of echinoderms. *Am. J. Sci.* **267**, 537–566 (1969).
39. Gorzelak, P., Stolarski, J., Mazur, M. & Meibom, A. Micro- to nanostructure and geochemistry of extant crinoid echinoderm skeletons. *Geobiology* **11**, 29–43 (2013).
40. O'Malley, C. E., Ausich, W. I. & Chin, Y.-P. Isolation and characterization of the earliest taxon-specific organic molecules (Mississippian, Crinoidea). *Geology* **41**, 347–350 (2013).
41. O'Malley, C. E., Ausich, W. I. & Chin, Y.-P. Deep echinoderm phylogeny preserved in organic molecules from Paleozoic fossils. *Geology* **44**, 379–382 (2016).
42. Tucker, M. E. & Wright, V. P. *Carbonate Sedimentology* (Blackwell Publishing Ltd., 1990).
43. Dickson, J. A. D. Diagenesis and crystal caskets: echinoderm Mg calcite transformation, Dry Canyon, New Mexico, U.S.A. *J. Sediment. Res.* **71**, 764–777 (2001).
44. Frank, T. D. & Lohmann, K. C. Diagenesis of fibrous magnesian calcite marine cement: implications for the interpretation of δ18O and δ13C values of ancient equivalents. *Geochim. Cosmochim. Acta* **60**, 2427–2436 (1996).
45. Levin, L., Hönisch, B. & Frieder, C. Geochemical proxies for estimating faunal exposure to ocean acidification. *Oceanography* **25**, 62–73 (2015).
46. Lebrato, M. et al. From the Arctic to the Antarctic: the major, minor, and trace elemental composition of echinoderm skeletons. *Ecology* **94**, 1434–1434 (2013).
47. Iglukowska, A., Humphreys-Williams, E., Przytarska, J., Chelchowski, M. & Kukliński, P. Minor and trace elements in skeletons of Arctic echinoderms. *Mar. Pollut. Bull.* **158**, 111377 (2020).
48. Yoshimura, T. et al. Altrivalent substitution of sodium for calcium in biogenic calcite and aragonite. *Geochim. Cosmochim. Acta* **202**, 21–38 (2017).
49. Laya, J. C. et al. Dissolution of ooids in seawater-derived fluids – an example from Lower Permian re-sedimented carbonates, West Texas, USA. *Sedimentology* **68**, 2671–2706 (2021).
50. Gierlowski-Kordesch, E. H. Lacustrine carbonates. *Dev. Sedimentol.* **61**, 1–101 (2010).
51. Tompa, É., Nyirő-Kósa, I., Rostási, Á., Cserny, T. & Pósfai, M. Distribution and composition of Mg-calcite and dolomite in the water and sediments of Lake Balaton. *Cent. Eur. Geol.* **57**, 113–136 (2014).
52. Chagas, A. A. P., Webb, G. E., Burne, R. V. & Southam, G. Modern lacustrine microbialites: towards a synthesis of aqueous and carbonate geochemistry and mineralogy. *Earth Sci. Rev.* **162**, 338–363 (2016).
53. Jones, B., Renaut, R. W. & Rosen, M. R. Trigonal dendritic calcite crystals forming from hot spring waters at Waikite, North Island, New Zealand. *J. Sediment. Res.* **70**, 586–603 (2000).
54. Ishikawa, M. & Ichikuni, M. Uptake of sodium and potassium by calcite. *Chem. Geol.* **42**, 137–146 (1984).
55. Devriendt, L. S. et al. Sodium incorporation into inorganic CaCO<sub>3</sub> and implications for biogenic carbonates. *Geochim. Cosmochim. Acta* **314**, 294–312 (2021).
56. Land, L. S. & Hoops, G. K. Sodium in carbonate sediments and rocks: a possible index to the salinity of diagenetic solutions. *J. Sediment. Res.* **43** (1973).
57. Hooker, J. D. & Binney, E. W. On the structure of certain limestone nodules enclosed in seams of bituminous coal, with a description of some Trigonocarpons contained in them. *Philos. Trans. R. Soc. Lond.* **145**, 149–156 (1855).

58. Weber, J. N. & Keith, M. L. Carbon-isotope composition and the origin of calcareous coal balls. *Science* **138**, 900–902 (1962).
59. Mozley, P. S. Relation between depositional environment and the elemental composition of early diagenetic siderite. *Geology* **17**, 704 (1989).
60. Lyons, P. C., Millay, M. A., Zodrow, E. L., Cross, A. T. & Gillis, K. S. Discovery of permineralized plant fossils (coal balls) in the Bolssovian (e.g., Westphalian C) (Middle Pennsylvanian, Upper Carboniferous), Stellarton Basin, Nova Scotia, Canada. *Can. J. Bot.* **73**, 1407–1416 (1995).
61. Lyons, P. C. et al. Coal-ball floras of Maritime Canada and palynology of the Foord seam: geologic, paleobotanical and paleoecological implications. *Rev. Palaeobot. Palynol.* **95**, 31–50 (1997).
62. Zodrow, E. L. & Cleal, C. J. Anatomically preserved plants in siderite concretions in the shale split of the Foord Seam: mineralogy, geochemistry, genesis (Upper Carboniferous, Canada). *Int. J. Coal Geol.* **41**, 371–393 (1999).
63. Whittaker, R. H. *Communities and Ecosystems* (Macmillan, 1975).
64. Bruenig, E. F. & Droste, H. J. Structure, Dynamics, and Management of Rainforests on Nutrient-Deficient Soils in Sarawakin in *Ecology, Conservation, and Management of Southeast Asian Rainforests* (eds. Primack, R. B. & Lovejoy, T. E.) Ch. 3, 41–53 (Yale University Press, 1995).
65. Cooper, H. V. et al. From peat swamp forest to oil palm plantations: the stability of tropical peatland carbon. *Geoderma* **342**, 109–117 (2019).
66. Ribeiro, R. de A., Rovai, A. S., Twilley, R. R. & Castañeda-Moya, E. Spatial variability of mangrove primary productivity in the neotropics. *Ecosphere* **10**, e02841 (2019).
67. Ravn, R. L. et al. Stratigraphy of the Cherokee Group and revision of Pennsylvanian stratigraphic nomenclature in Iowa *Iowa Geol. Surv. Tech. Inform. Ser.* **12**, 1–76 (1984).
68. Raymond, A. The paleoecology of a coal-ball deposit from the middle Pennsylvanian of Iowa dominated by cordaitalean gymnosperms. *Rev. Palaeobot. Palynol.* **53**, 233–250 (1988).
69. DiMichele, W. A. & Phillips, T. L. Paleobotanical and paleoecological constraints on models of peat formation in the Late Carboniferous of Euramerica. *Palaeogeogr. Palaeoclimatol. Palaeoecol.* **106**, 39–90 (1994).
70. Raymond, A., Lambert, L., Costanza, S., Slone, E. J. & Cutlip, P. C. Cordaites in paleotropical wetlands: an ecological re-evaluation. *Int. J. Coal Geol.* **83**, 248–265 (2010).
71. Lane, S. J. & Dalton, J. A. Electron microprobe analysis of geological carbonates. *Am. Mineral.* **79**, 745–749 (1994).
72. Macqueen, R. W. & Ghent, E. D. Electron microprobe study of magnesium distribution in some Mississippian echinoderm limestones from western Canada. *Can. J. Earth Sci.* **7**, 1308–1316 (1970).
73. Reed, S. J. B. *Electron Microprobe Analysis and Scanning Electron Microscopy in Geology* (Cambridge Univ. Press, 2005).
74. Richter, D. K. & Fuchtbauer, H. Ferroan calcite replacement indicates former magnesian calcite skeletons. *Sedimentology* **25**, 843–860 (1978).
75. Hasiuk, F. J. & Lohmann, K. C. Application of calcite Mg partitioning functions to the reconstruction of paleocean Mg/Ca. *Geochim. Cosmochim. Acta* **74**, 6751–6763 (2010).
76. Alderton, D. Carbonates (Ca, Mg, Fe, Mn) in *Encyclopedia of Geology* (eds. Alderton, D. & Elias, S. A.) 382–394 (Elsevier Science, 2020).
77. Campbell, R. C. *Statistics for Biologists* (Cambridge Univ. Press, 1989).

## Acknowledgements

Discussions with R. Guillemette, B. Wilkinson and W. A. DiMichele contributed to this paper. R. Wells, J. Teoh and A. Mott assisted with SEM images and electron microscopy (RRID:SCR\_022202). C. Scotese consulted on the paleogeographic reconstruction in Fig. 1. Student research grants to M. Chrapa from GSA and GSA Energy Division (Antoinette Lierman Medlin Scholarship) supported this research. No permissions were required for the Dalton or Calhoun samples. We would like to thank the reviewers and Editors for their thoughtful comments and efforts towards improving our manuscript.

## Author contributions

M.E.C. and A.R. conceived the idea, collected samples, processed data, performed statistical analysis, wrote the paper, and created figures/tables. M.E.C., A.R., and W.M.L. prepared samples. All authors performed geochemical analyses. J.-C.L. and W.M.L. assisted with data interpretation and discussion. W.M.L. assisted with Methods.

## Competing interests

The authors declare no competing interests.

## Additional information

**Supplementary information** The online version contains supplementary material available at <https://doi.org/10.1038/s43247-023-00876-5>.

**Correspondence** and requests for materials should be addressed to Michelle E. Chrapa.

**Peer review information** *Communications Earth & Environment* thanks Gregory Retallack, Przemyslaw Gorzelak, Blaine Cecil, and the other, anonymous, reviewer(s) for their contribution to the peer review of this work. Primary Handling Editors: Olivier Sulpis and Joe Aslin.

**Reprints and permission information** is available at <http://www.nature.com/reprints>

**Publisher's note** Springer Nature remains neutral with regard to jurisdictional claims in published maps and institutional affiliations.



**Open Access** This article is licensed under a Creative Commons Attribution 4.0 International License, which permits use, sharing, adaptation, distribution and reproduction in any medium or format, as long as you give appropriate credit to the original author(s) and the source, provide a link to the Creative Commons license, and indicate if changes were made. The images or other third party material in this article are included in the article's Creative Commons license, unless indicated otherwise in a credit line to the material. If material is not included in the article's Creative Commons license and your intended use is not permitted by statutory regulation or exceeds the permitted use, you will need to obtain permission directly from the copyright holder. To view a copy of this license, visit <http://creativecommons.org/licenses/by/4.0/>.

© The Author(s) 2023